Progress In Electromagnetics Research M, Vol. 90, 27–35, 2020

Terahertz Beam Splitter Based on I-Shaped Metasurface

Wu Pan, Xueyin Wang*, Qi Chen, Xinyu Ren, and Yong Ma

Abstract—A linear polarization beam splitter operating in terahertz band is proposed and experimentally verified in this paper. The unit cell of the beam splitter is composed of the top "I" type metal pattern, the middle dielectric layer, and the bottom metal layer. Each subarray structure of the device consists of four unit cells that rotate progressively at an angle of 45°. The horizontal and vertical sub-arrays form the gradient metasurface of 4×4. The incident linear polarized terahertz wave is reflected by the device and divided into four beams with approximately equal power, while having different propagating directions in the 0.18–0.30 THz band. The proposed terahertz beam splitter has the advantages of small size, low cost, and easy processing, and it can be applied to terahertz stealth and terahertz imaging.

1. INTRODUCTION

Terahertz (THz) technology, as one of the advanced technologies in the present world, has been widely used in medicine, radar, communications, military, aerospace, astronomical observation, and other fields, and it was named as one of the "Ten Technologies that change the world" by the United States in 2014. Beam splitting control of terahertz wave is one of the key research contents of terahertz science and technology [1, 2]. Terahertz beam splitter is the basic device of a terahertz system, which is widely used in coherent terahertz measurement systems and structural analysis of complex organic materials [3]. With the rapid development of terahertz technology, there is a great demand for high efficiency, flexibility and low-cost terahertz beam splitters. Usually, terahertz beam splitters are made of wire mesh, thin film, and silicon substrate [4, 5], but they require tilted terahertz wave incidence and complex manufacturing processes. In addition, the traditional terahertz beam splitter is too bulky to be miniaturized. The recent emergence of metasurface offers new opportunities for planarization of terahertz devices [6–11]. Many scholars have constructed terahertz devices using metasurface to manipulate terahertz waves more conveniently. The metasurface has very good application prospects in polarization conversion, polarization preservation, imaging, and beam isolation of terahertz wave [12–15]. In 2015, Gao et al. [16] proposed a method for encoding a metasurface beam splitter. At 0.8–2.0 THz, the vertically incident terahertz wave can be divided into different numbers of reflected beams under different coding conditions. In 2016, Headland et al. [17] proposed a reflective beam splitter. The beam splitter splits the incident wave into two beams with a variable angle. In 2017, Wei et al. [18] proposed and designed an all dielectric metasurface terahertz beam splitter. Simulation and measurement results show that in the range of 0.6–1.0 THz, the incident terahertz wave can be split into two beams. We can continuously adjust the split ratio by simply moving the metasurface, and we can also adjust the exit angle by selecting the step of the phase gradient. In 2017, Lee et al. [19] designed a reflective terahertz circular polarization beam splitter which divides the incident circularly polarized wave into left-handed and right-handed circularly polarized waves, covering the band of 0.58–1.00 THz. In 2018, Yi et al. [20]

Received 28 October 2019, Accepted 6 January 2020, Scheduled 19 February 2020

* Corresponding author: Xueyin Wang (xueyinw88@163.com).

The authors are with the College of Photoelectric Engineering, Chongqing University of Posts and Telecommunications, Chongqing 400065, China.

designed a metasurface that controls the terahertz wavefront. Using the metasurface, the terahertz wave is reflectively divided into two waves in the band of 0.22–0.30 THz, and their deflection angle can be effectively controlled, and this device can be applied as beam splitters in low-cost and compact terahertz imaging systems. In 2018, Zhang et al. [21] designed a reflective terahertz metasurface beam splitter. The metasurface is formed by metal rods in different directions on polyimide film. It can split the reflected beam into four beams of nearly the same density under the illumination of linearly polarized terahertz waves in the 0.8–1.4 THz band. In 2019, Jia et al. [22] designed a circular polarization terahertz beam splitter. In the range of 0.3–1.0 THz, the incident circularly polarized waves can be divided into left-handed and right-handed circularly polarized waves, and their deflection angle can be effectively controlled. The beam splitter can be used in biological imaging and low-cost terahertz imaging systems.

2. DESIGN OF A METASURFACE CELL

The unit cell for the reflective beam splitter has three layers as shown in Figure 1. An "I" pattern of gold with a thickness of 0.002 mm makes up the top layer of the unit cell. The middle layer is 0.254 mm thick and composed of low loss Duroid 5880 which has a relative permittivity $\varepsilon_r = 2.3$ and loss tangent [23] $\tan\delta = 0.02$. The bottom plane is a gold layer with a thickness of 0.002 mm. The top pattern dimensions are $l = 0.320$ mm, $w = 0.100$ mm, $g = 0.200$ mm, $a = 0.700$ mm. Electromagnetic resonance occurs between the top metal layer and bottom metal layer, resulting in a phase change of the reflected wave [24].

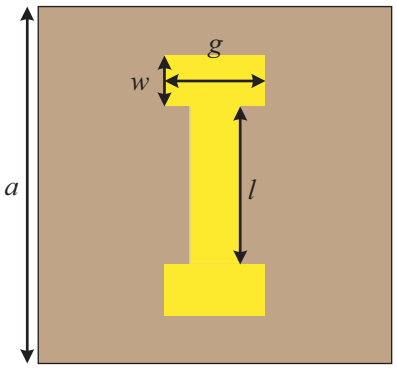

Figure 1. Schematic diagram of the unit cell. The dimensions are as follows: $l = 0.320$ mm, $w = 0.100$ mm, $g = 0.200$ mm, $a = 0.700$ mm.

3. METASURFACE ANALYSIS AND DESIGN

For the purpose of dividing terahertz into multiple beams by using metasurface, a terahertz beam splitter that is thin, easy-to-machine, multi-splitting, and variable reflection angle is proposed in this paper. The schematic of metasurface-based multi-splitting terahertz beam splitter is shown in Figure 2. A linearly polarized terahertz beam incident on the sample is divided into four beams at different directions.

The propagation process of terahertz waves and its geometric phases generation in the metasurface can be described by using Jones matrix. The incident linearly polarized terahertz beam can be considered as the superposition of two circularly polarized beams with opposite helicities [25], which can be written as

$$\begin{bmatrix} 1 \\ 0 \end{bmatrix} = \frac{1}{2}\left(\begin{bmatrix} 1 \\ i \end{bmatrix} + \begin{bmatrix} 1 \\ -i \end{bmatrix} \right). \tag{1}$$

In order to realize a beam splitter that splits the outgoing wave into four beams, we design both x and y directions to have a phase gradient and satisfy the phase coverage of 2π. Therefore, when the linearly polarized terahertz wave interacts with the reflective metasurface, it is divided into four beams with the designed angle. The phase distribution of terahertz wave required on x-axis is descried as [26]:

$$\Phi(x) = \arg\left(\exp(i\delta_x) + \exp(-\delta_x)\right). \tag{2}$$

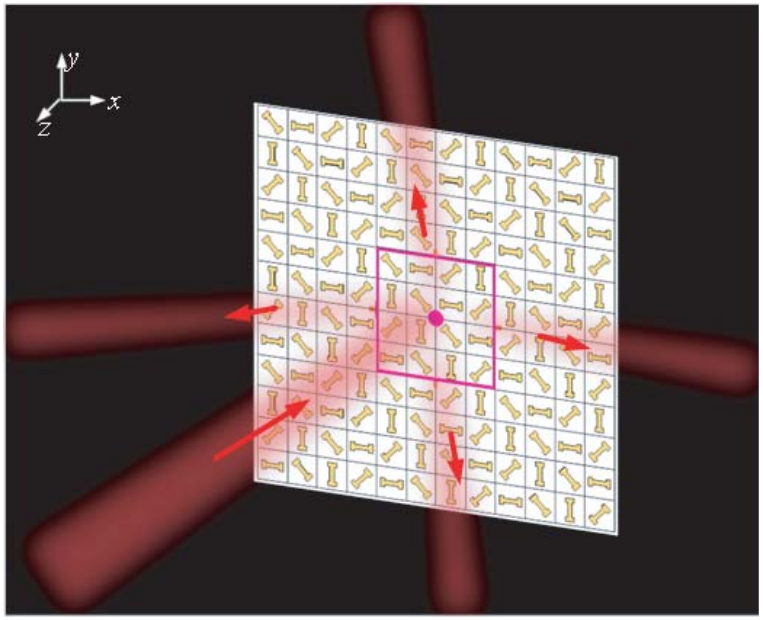

Figure 2. Schematic of the metasurface-based multi-splitting terahertz beam splitter.

Accordingly, the total phase distribution of terahertz wave is governed by:

$$\Phi(x,y) = \arg\left\{\exp(i\delta_x) + \exp(-i\delta_x) + \exp(i\delta_y) + \exp(-i\delta_y)\right\}, \tag{3}$$

where $\pm\delta_x$ and $\pm\delta_y$ are phase gradients along x and y axes, respectively. The device can be degraded into four channels of the beam splitter.

The generalized Snell's law of reflection is revisited by introducing an abrupt phase shift at the interface between the two media. Assume that the phase difference between terahertz waves traveling along the actual path ABC and AEC is zero [27], as shown in Figure 3. It has the following relationship:

$$(k_0 n_i \sin\theta_r \mathrm{d}x + \Phi + \mathrm{d}\Phi) - (k_0 n_r \sin\theta_r \mathrm{d}x + \Phi) = 0, \tag{4}$$

where θ_i and θ_r are the incident and reflection angles of terahertz wave, respectively; Φ and $\Phi + \mathrm{d}\Phi$ are the phase discontinuities where two electromagnetic waves pass through the interface; $k = 2\pi/\lambda$, λ is the wavelength in vacuum; k is the electromagnetic wave number in free space; n_i is the refractive index of the incident media; dx is the distance between point B and point E at the incident interface; $\mathrm{d}\Phi/\mathrm{d}x = \Delta\Phi$ is the phase difference along the interface. If $\Delta\Phi$ is constant, the generalized Snell's law

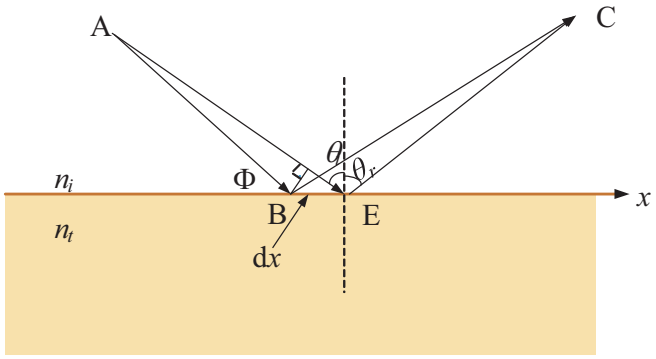

Figure 3. Generalized Snell's law diagram on the interface.

of reflection can be derived from Equation (4), as shown in the following equation:

$$\sin\theta_r - \sin\theta_i = \frac{\lambda_0}{2\pi n_i}\Delta\Phi. \tag{5}$$

According to Equation (5), the reflection direction of terahertz wave can be controlled by choosing an appropriate constant $\Delta\Phi$. Assuming that the unit cell size is a, the reflection angle of the terahertz wave incident on the surface is θ_r, then the gradient of phase discontinuity can be expressed as:

$$\Delta\Phi = -k_0 a \sin\theta_r. \tag{6}$$

Therefore, the reflection angle θ_r is only related to $\Delta\Phi$. For the metasurface, the unit cell under the incident of the terahertz wave is periodically rotated, where $\Delta\Phi = 2\pi/N$ (N is the number of unit cells contained in each cycle) [28]. The reflection angle of the terahertz wave can be calculated by using the following equation:

$$\theta_r = \arcsin\left(\frac{\lambda}{Na}\right). \tag{7}$$

The relationship between gradient of phase discontinuity $\Delta\Phi$ and rotation angle between adjacent units is $\Delta\Phi = 2\beta$, then the phase gradient expression can be written as:

$$\nabla\Phi = \frac{\pm 2\beta}{a}, \tag{8}$$

The same phase gradient is designed in x and y directions, as follows:

$$\nabla\Phi_x = \nabla\Phi_y = \pi/2. \tag{9}$$

Four unit cells of 0°, 45°, 90°, and 135° were designed as a subarray. Rotation angle $\beta = \pi/4$, and phase difference between adjacent units $\Delta\Phi = \pi/2$. As shown in Figure 4, one subarray covers a phase gradient of 2π. Both the horizontal and vertical axis subarrays of the metasurface are designed to satisfy 2π phase coverage. A reflective terahertz beam splitter is constructed from a 4×4 phase gradient metasurface. The beam splitter splits the incident terahertz wave into four beams and has different angles of reflection in the operating frequency band.

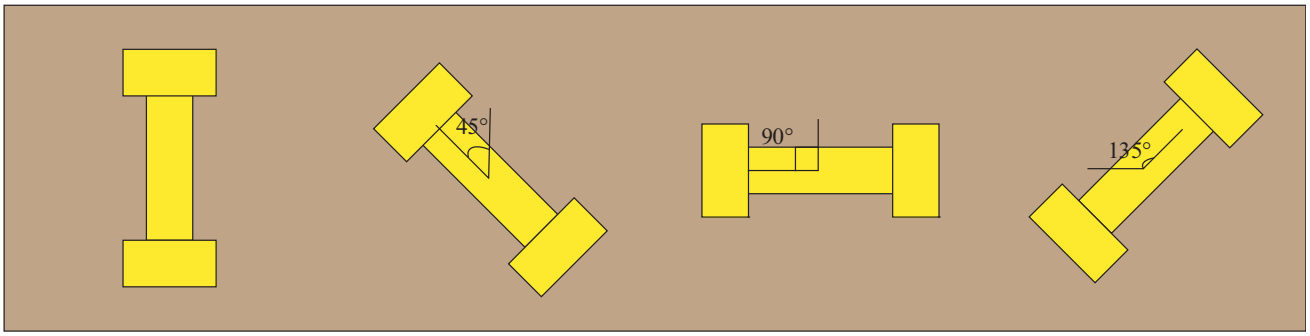

Figure 4. Subarray design for beam splitter.

From Equation (7), it can be concluded that $\theta_1 \approx 38°$ at $f_1 = 0.18\,\text{THz}$, $\theta_2 \approx 27°$ at $f_2 = 0.24\,\text{THz}$, and $\theta_3 \approx 21°$ at $f_3 = 0.30\,\text{THz}$. It can be seen that the reflection angle is different in the operating frequency band, and the reflection angle decreases as the frequency increases.

4. RESULTS

The designed beam splitter is simulated by the frequency-domain solver of CST Microwave Studio. In order to simulate an infinite gradient array, the periodic boundary conditions is set in the x-y plane and the free space environment set in the opposite direction to the z-axis. Figure 5 shows the reflectivity

curve of the metasurface. It can be seen from the figure that for a normal incident wave, there is a reflection trough at the center frequency $f = 0.24$ THz of the design, corresponding to an absorption peak. At this time, the incident wave is efficiently coupled into the surface wave, and the reflectivity is lowered. However, for the linearly polarized incident wave, the frequency of the minimum reflectance is slightly offset from the center frequency, mainly due to the calculation of the reflected phase. When using periodic boundary conditions, the coupling between units is strong. After the phase gradient metasurface is formed, the adjacent units have different structural dimensions, and their coupling between the periodic units is weakened relative to the calculation of the reflected phase. Therefore, there is a certain deviation between the actual phase gradient and the designed phase gradient. The phase differences between adjacent small cells in the designed metasurface cell structure are no longer equal, and there is no unique phase gradient in the x and y directions, thus generating abnormal

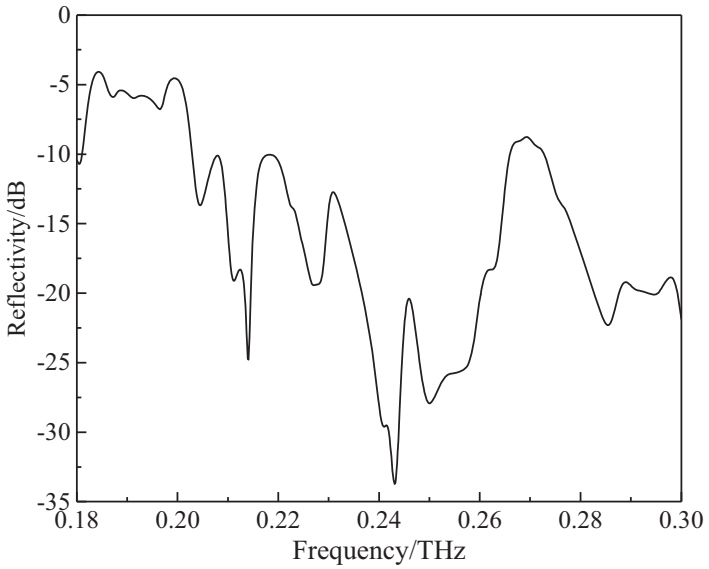

Figure 5. Reflectivity simulation result.

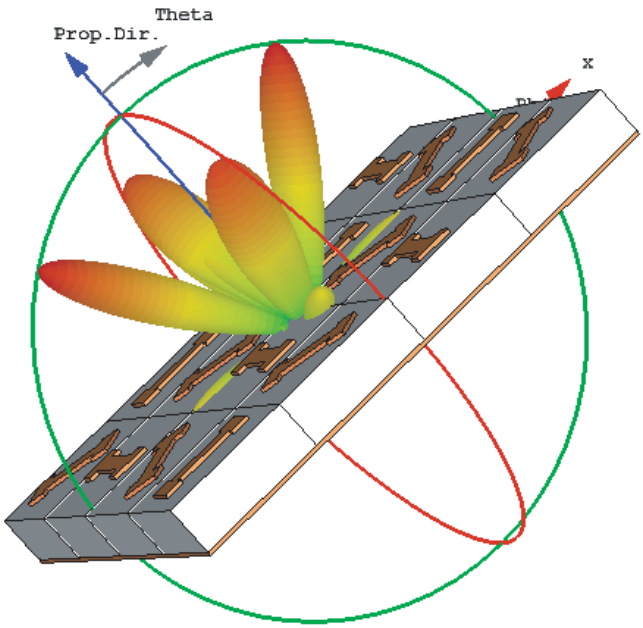

Figure 6. 3D far-field pattern of the metasurface.

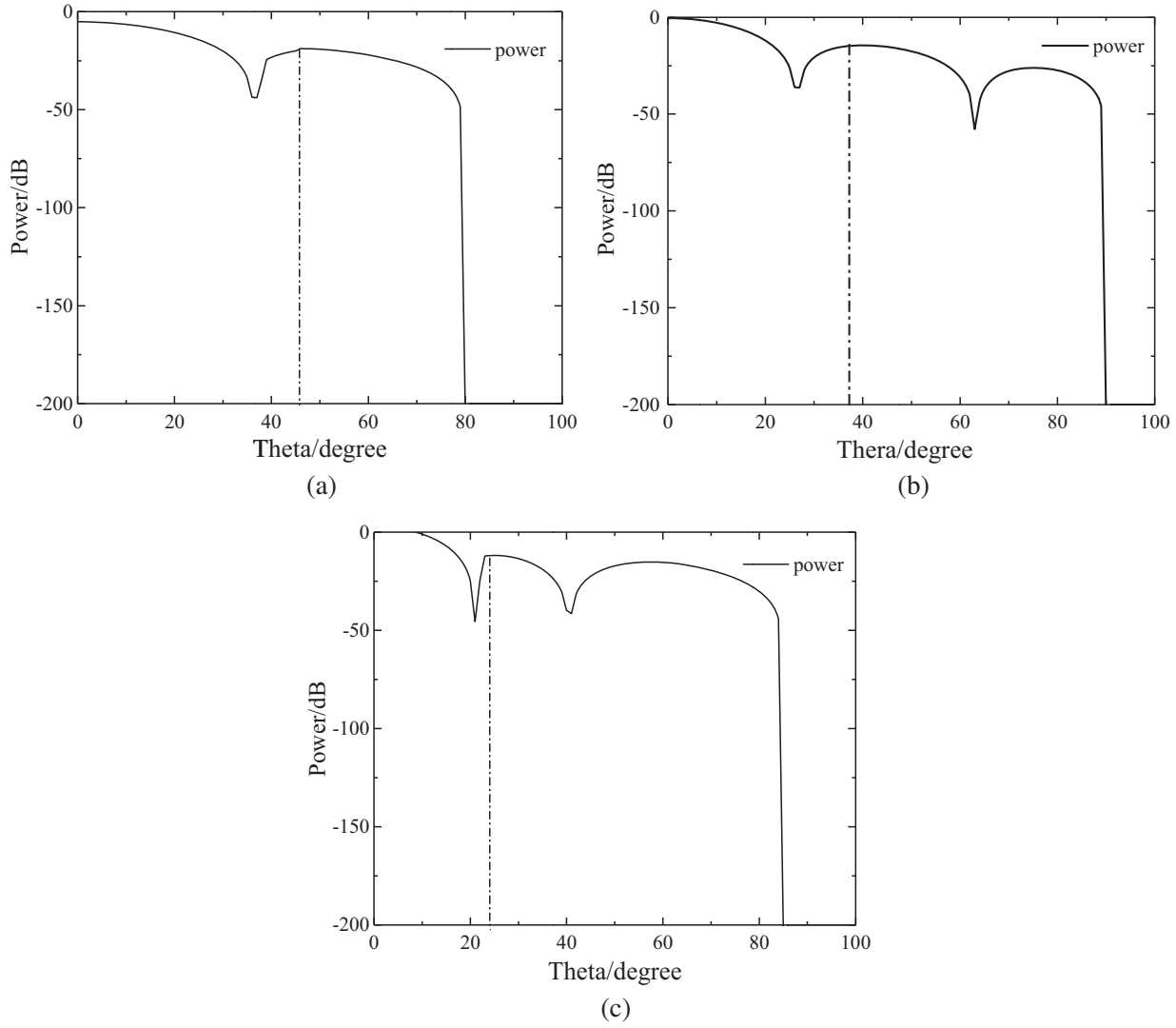

Figure 7. Cartesian diagram of different frequency waves normally incident on metasurface. (a) $f_1 = 0.18\,\text{THz}$. (b) $f_2 = 0.24\,\text{THz}$. (c) $f_3 = 0.30\,\text{THz}$.

reflection, resulting in a decrease in reflectivity.

Figure 6 shows the 3D far-field pattern of the metasurface in which the improvements of gain against the patch cell and beam splitting are obtained. The incident wave is reflected into four waves of equal energy and different propagation directions, and the four beams are located on the $\pm x$ and $\pm y$ axes, respectively.

In order to obtain the angles of the reflected beams, numerical results are shown in Figure 7 which is a Cartesian diagram of the terahertz wave incident on the metasurface at phi = 45°. The degree at the maximum sidelobe power is the angle of the reflected wave, and the dashed line in the figure corresponds to the reflection angle of the frequency point. It can be seen that $\theta_1 \approx 45°$ at $f_1 = 0.18\,\text{THz}$, $\theta_2 \approx 34°$ at $f_2 = 0.24\,\text{THz}$, and $\theta_3 \approx 24°$ at $f_3 = 0.30\,\text{THz}$. Obviously, the simulation refraction angles are in good accordance with the theoretical ones calculated by the general refraction law. Besides, there is a slight difference in realized gain between the splitting beams, which is due to different effective apertures.

Furthermore, the beam number and exit angle of different beam splitters which were mentioned previously have been compared with our presented structure in Table 1. It is found that the proposed beam splitter reaches a relatively high number of beams and meets a variable exit angle as compared

Table 1. Comparison with some other reported terahertz beam splitters.

Beam splitter	Working frequency	Beam number	Exit angle
Gao et al. [16]	0.8–2.0 THz	variable	invariable
Headland et al. [17]	1 THz	2	variable
Wei et al. [18]	0.6–1.0 THz	2	variable
Lee et al. [19]	0.58–1.00 THz	2	variable
Yi et al. [20]	0.22–0.30 THz	2	invariable
Zhang et al. [21]	0.8 ∼ 1.4 THz	4	variable
Jia et al. [22]	0.3–1.0 THz	2	variable
proposed coupler	0.18–0.30 THz	4	variable

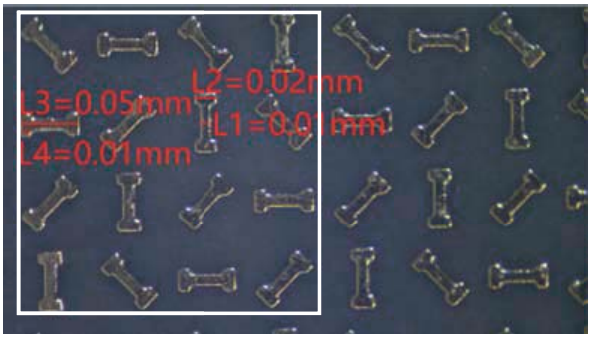

Figure 8. The fabricated metasurface beam splitter sample.

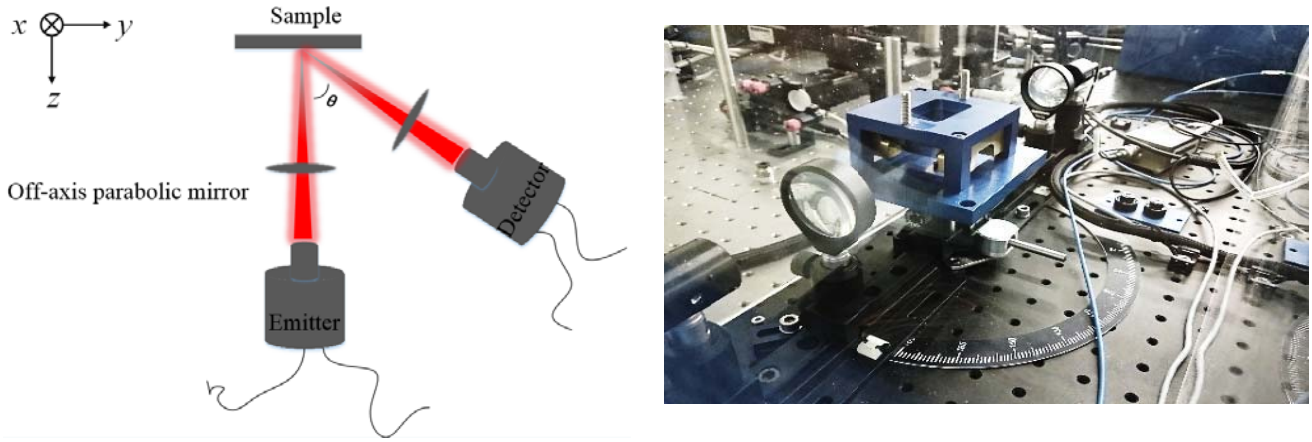

(a) (b)

Figure 9. Measurement system to measure the beam splitter. (a) Schematic diagram. (b) Photograph.

to [17–23].

To further validate our design, a sample (size: 56 mm × 56 mm) is fabricated using printed circuit board technology, as shown in Figure 8, where the inset is a magnified view of a single "super-unit" structure.

The experiment platform shown in Figure 9 is used to experimentally verify the properties of the designed beam splitter. Here, two fiber-based terahertz photoconductive antennas are mounted on the rotatable stage, one of which is employed as a transmitter, and the other is a receiver. The powers of

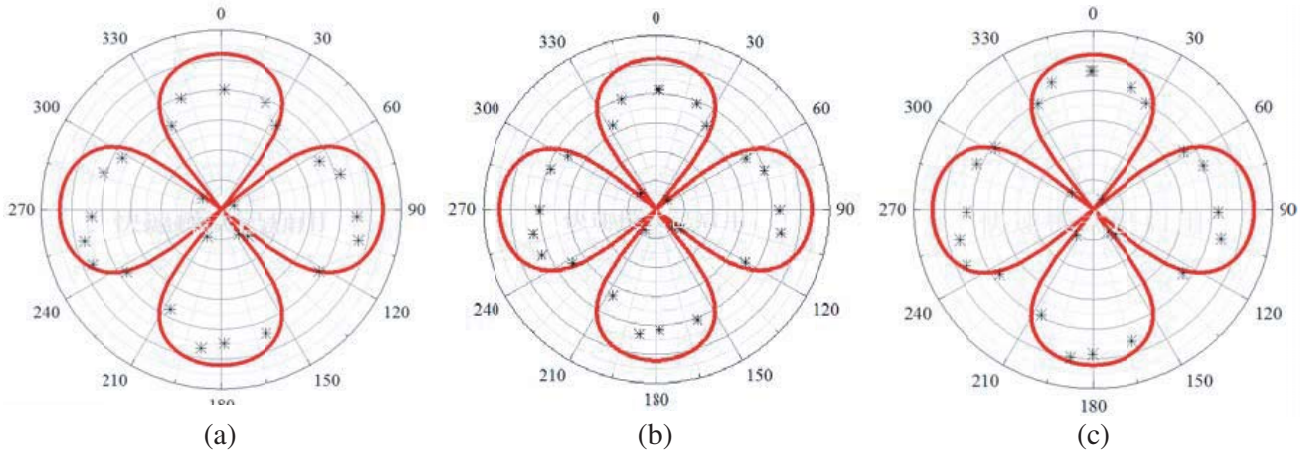

Figure 10. Simulated (solid curves) and experimentally measured (discrete asterisks) power distribution (along with angle) of the terahertz beam splitter. (a) 0.186 THz, 35°. (b) 0.236 THz, 27°. (c) 0.299 THz, 20°.

the different points are measured by rotating the detector around the semi-circle circumference.

The power distribution and angle of the reflected beam are shown in Figure 10. The measured range of angles covers 20° to 40° for reflected waves, corresponding to a frequency range of 0.30–0.18 THz. Therefore, it can be inferred that under the illumination of a linearly polarized terahertz wave, the reflected beam is divided into four beams of approximately equal power with different propagation directions in the operating frequency band. The experimental results are basically consistent with the simulated results. The difference between the experimental and simulation results is mainly due to the fabrication error of the device and the attenuation of terahertz wave in the air during the measurement.

5. CONCLUSION

A method of the reflective terahertz beam splitter operating in the 0.18–0.30 THz band is proposed. The incident terahertz wave is reflected and divided into four beams with approximately equal power. Different frequency points have different reflection angles. The designed terahertz beam splitter not only has a wide range of applications in terahertz imaging, stealth, and other fields but also provides a new way for device miniaturization and system integration. The terahertz beam splitter can be used for wavelength division multiplexing in future high-speed terahertz communication systems.

ACKNOWLEDGMENT

This work was supported by New Direction Cultivation Project of Chongqing University of Posts and Telecommunications (A2014-116); the Key Research Program of Chongqing University of Posts and Telecommunications on Interdisciplinary and emerging field (A2018-01).

REFERENCES

1. Li, J. S., D. G. Xu, and J. Q. Yao, "Compact terahertz wave polarizing beam splitter," *Applied Optics*, Vol. 49, No. 24, 4494–4497, 2010.
2. Gao, X., L. Zhou, X. Y. Yu, et al., "Ultra-wideband surface plasmonic Y-splitter," *Optics Express*, Vol. 23, No. 18, 23270–23277, 2015.
3. Rizea, A., "Design technique for all-dielectric non-polarizing beam splitter plate," *Opto-Electronics Review*, Vol. 20, No. 1, 96–99, 2012.
4. Berry, C. W., J. Moore, and M. Jarrahi, "Design of reconfigurable metallic slits for terahertz beam modulation," *Optics Express*, Vol. 19, No. 2, 1236–1245, 2011.

5. Berry, C. W. and M. Jarrahi, "Broadband terahertz polarizing beam splitter on a polymer substrate," *Journal of Infrared, Millimeter and Terahertz Waves*, Vol. 33, No. 2, 127–130, 2012.
6. Guo, W. L., G. M. Wang, H. P. Li, et al., "A novel broadband gradient metasurface," *Journal of Microwaves*, Vol. 32, No. 3, 51–54, 2016.
7. Yu, N., F. Aieta, P. Genevet, et al., "A broadband, background-free quarter-wave plate based on plasmonic metasurfaces," *Nano Letters*, Vol. 12, No. 12, 6328–6333, 2012.
8. Grady, N. K., J. E. Heyes, D. R. Chowdhury, et al., "Terahertz metamaterials for linear polarization conversion and anomalous refraction," *Science*, Vol. 340, No. 6138, 1304–1307, 2013.
9. Yang, B., W. M. Ye, X. D. Yuan, et al., "Design of ultrathin plasmonic quarter-wave plate based on period coupling," *Optics Letters*, Vol. 38, No. 5, 679–681, 2013.
10. Fan, R. H., Y. Zhou, X. P. Ren, et al., "Freely tunable broadband polarization rotator for terahertz waves," *Advanced Materials*, Vol. 27, No. 7, 1201–1206, 2015.
11. Scherger, B., C. Jördens, and M. Koch, "Variable-focus terahertz lens," *Optics Express*, Vol. 19, No. 5, 4528–4535, 2011.
12. Jiang, X. Y., J. S. Ye, J. W. He, et al., "An ultrathin terahertz lens with axial long focal depth based on metasurfaces," *Optics Express*, Vol. 21, No. 24, 30030–30038, 2013.
13. Cong, L., W. Cao, X. Zhang, et al., "A perfect metamaterial polarization rotator," *Applied Physics Letters*, Vol. 103, No. 17, 171107–171112, 2013.
14. Cong, L., N. Xu, J. Gu, et al., "Highly flexible broadband terahertz metamaterial quarter-wave plate," *Laser & Photonics Reviews*, Vol. 8, No. 4, 626–632, 2014.
15. Shi, H., J. Li, A. Zhang, et al., "Gradient metasurface with both polarization-controlled directional surface wave coupling and anomalous reflection," *IEEE Antennas and Wireless Propagation Letters*, Vol. 14, 104–107, 2015.
16. Gao, L. H., Q. Cheng, J. Yang, et al., "Broadband diffusion of terahertz waves by multi-bit coding metasurfaces," *Light: Science & Applications*, Vol. 4, No. 9, 324–332, 2015.
17. Headland, D., T. Niu, E. Carrasco, et al., "Terahertz reflectarrays and nonuniform metasurfaces," *IEEE Journal of Selected Topics in Quantum Electronics*, Vol. 23, No. 4, 1–18, 2016.
18. Wei, M., Q. Xu, Q. Wang, et al., "Broadband non-polarizing terahertz beam splitters with variable split ratio," *Applied Physics Letters*, Vol. 111, No. 7, 071101–071104, 2017.
19. Lee, W. S. L., S. Nirantar, D. Headland, et al., "Broadband terahertz circular-polarization beam splitter," *Advanced Optical Materials*, Vol. 6, No. 3, 1700852, 2017.
20. Yi, H., S. W. Qu, K. B. Ng, et al., "Terahertz wavefront control on both sides of the cascaded metasurfaces," *IEEE Transactions on Antennas and Propagation*, Vol. 66, No. 1, 209–216, 2018.
21. Zhang, X. F., H. H. Gong, Z. Li, et al., "Metasurface for multi-channel terahertz beam splitters and polarization rotators," *Applied Physics Letters*, Vol. 112, No. 17, 171111–171115, 2018.
22. Jia, M., Z. Wang, H. Li, et al., "Efficient manipulations of circularly polarized terahertz waves with transmissive metasurfaces," *Light: Science & Applications*, Vol. 8, No. 1, 16–24, 2019.
23. Sun, Y. Y., L. Han, X. Y. Shi, et al., "General laws of reflection and refraction for metasurface with phase discontinuity," *Acta Phys. Sin.*, Vol. 62, No. 10, 104201–104208, 2013.
24. Yue, F., C. Zhang, X. F. Zang, et al., "High-resolution grayscale image hidden in a laser beam," *Light: Science & Applications*, Vol. 7, No. 1, 17129–17134, 2018.
25. Shi, H., J. Li, A. Zhang, et al., "Gradient metasurface with both polarization-controlled directional surface wave coupling and anomalous reflection," *IEEE Antennas and Wireless Propagation Letters*, Vol. 14, 104–107, 2015.
26. Zang, X. F., F. Dong, F. Yue, et al., "Polarization encoded color image embedded in a dielectric metasurface," *Advanced Materials*, 1707499, 2018.
27. Ng, K. B., C. H. Chan, et al., "On the dielectric properties of substrates with different surface conditions for submillimeter-wave and terahertz applications," *THz Sci. Technol.*, Vol. 9, No. 2, 45–59, 2016.
28. Han, L. and Z. H. Wang, "Two methods for general laws of reflection and refraction," *College Physics*, Vol. 32, No. 3, 49–52, 2013.